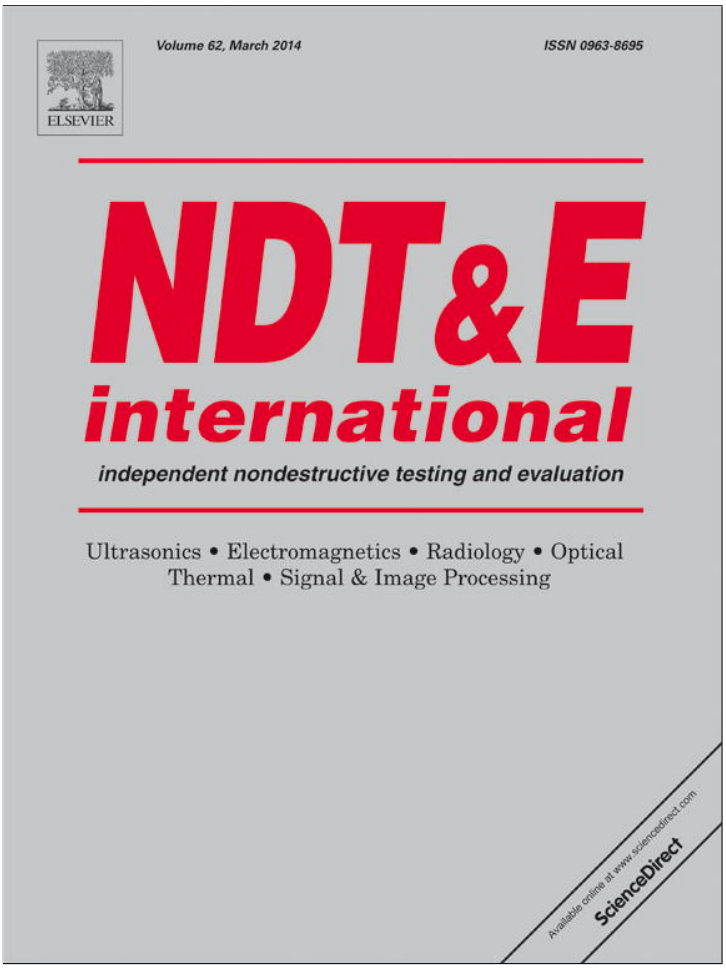

NDT&E International 62 (2014) 122–129

Contents lists available at ScienceDirect

NDT&E International

journal homepage: www.elsevier.com/locate/ndteint

Micro-crack detection using a collinear wave mixing technique

Jingpin Jiao *, Junjun Sun, Nan Li, Guorong Song, Bin Wu, Cunfu He

Beijing University of Technology, Ping Le Yuan 100#, Chaoyang District, Beijing 100124, China

ARTICLE INFO

Article history:
Received 27 February 2013
Received in revised form
19 November 2013
Accepted 17 December 2013
Available online 27 December 2013

Keywords:
Frequency mixing
Micro-crack
Nonlinear ultrasound
Bispectrum
Ultrasonic intermodulation

ABSTRACT

A collinear wave mixing technique was developed to detect micro-cracks in samples by measuring the mixing of two ultrasonic sinusoidal waves. The bispectrum was used to process the nonlinear response. Experiments were conducted to investigate the influence of excitation parameters, such as driving frequency and time delay, on intermodulation among ultrasonic waves and defects. Mixing components were tracked for varying frequency or time delay, and the nonlinear response was measured at fixed frequencies and time delay. The driving frequency was found to strongly affect micro-crack detection; the optimal driving frequency corresponded to maximum amplitudes of sum and difference frequency sidebands. The time-delay dependence of the amplitude of mixing components allowed the location of defects throughout a sample.

1. Introduction

The use of ultrasound is one of the most powerful techniques available to detect and characterize defects in materials and structures. The conventional ultrasonic technique is based on the phenomenon of reflection or transmission and is therefore sensitive to gross defects and open cracks. However, for the detection of micro-cracks or degradation, the conventional ultrasonic technique has quite low sensitivity. The use of nonlinear ultrasonic techniques has been found to be promising in overcoming this problem [1,2].

The most common methods of measuring the nonlinearity in solids are those based on the acoustoelastic effect [3,4], harmonic generation [5–7] and wave mixing [8,9]. The acoustoelastic method measures acoustic velocity variations induced by damage to structures. However, the approach is limited by the difficulty of measuring the small changes in acoustic velocity in practice. The most classical phenomenon employed in measuring nonlinearity is harmonic generation, where the waveform of an incident wave is distorted by the nonlinear elastic response of the medium to finite-amplitude waves. However, practical implementation of the harmonic method requires much effort to minimize nonlinear distortions in transmitting/receiving devices.

The wave mixing method is based on the fact that a resonant wave might be generated by two incident waves if certain conditions are satisfied. The generated resonant wave is related to the nonlinearity of materials/structures. Therefore, by measuring the generated resonant wave, the nonlinearity might be obtained. The wave mixing technique has two important advantages over the conventional nonlinear ultrasonic harmonic generation technique: it is less sensitive to nonlinearities in the measurement system and it allows for great flexibility in selecting the wave modes, frequencies, and propagating directions [10,11].

According to the incident directions of two ultrasonic waves, a wave mixing method can be classified as collinear wave mixing and non-collinear wave mixing. Recent research suggests that these methods have promise as nondestructive testing techniques. Croxford et al. reported the application of a non-collinear mixing technique to the ultrasonic measurement of material nonlinearity to assess plasticity and fatigue damage [12,13]. The linear ultrasonic measurement technique and the non-collinear ultrasonic wave mixing technique have been used to detect the physical ageing of polyvinyl chloride [14]. It was demonstrated experimentally that linear ultrasonic parameters, such as velocity dispersion and attenuation, were insensitive to the physical ageing state of polyvinyl chloride. However, the non-collinear ultrasonic wave mixing process does lead to significant sensitivity to the physical ageing of polyvinyl chloride, which has been verified experimentally in the laboratory and field. Jacob [15] applied the collinear mixing technique to measure the nonlinearity parameter for various solids. Since the determination of the nonlinearity parameter is based on the measurement of the phase modulation, the measurement was absolute and the uncertainty was small. Liu [16] introduced a new acoustic nonlinearity parameter associated with the interaction between a longitudinal wave and a shear wave in isotropic elastic solids. Experimental measurements were conducted to demonstrate that the collinear wave mixing technique is capable of measuring plastic deformation in Al-6061 alloys. These

* Corresponding author. Tel.: +86 1067391720.
E-mail address: jiaojp@bjut.edu.cn (Jingpin Jiao).

0963-8695/$ - see front matter © 2013 Elsevier Ltd. All rights reserved.
http://dx.doi.org/10.1016/j.ndteint.2013.12.004

results indicate that collinear wave mixing is a promising method for nondestructive assessment of plastic deformation, and possibly, fatigue damage in metallic materials. Hills [17,18] and Courtney [19] developed a special collinear wave mixing technique for global crack detection in structures. The main difference in their technique was that the two sinusoidal signals were applied to the same transmitter. To isolate the sideband at the sum or difference frequency, the received signal was processed employing bispectral analysis. The bispectrum was shown to be particularly useful in extracting the nonlinearity related to phase coupling. Courtney [20] thoroughly discussed how the sensitivity of the technique depends on the frequencies and amplitudes of the applied signals, the positions of the transducers and the support conditions. In this work, the collinear waves mixing technique is used to detect fatigue cracks in metal, and the nonlinear response of the samples to continuous excitations at two frequencies is processed using the well-known bispectrum method. The research focuses on the experimental effects of excitation parameters, such as the driving frequency and time delay, on the intermodulation of ultrasonic waves and defects.

2. Bispectrum analysis for nonlinearity characterization in wave mixing

As a nonlinear element, a defect can transform part of the incident acoustic energy into nonlinear acoustic waves with different frequencies (harmonics and combination frequencies), effectively becoming a source of nonlinear acoustic waves. Therefore, an elastic structure with a defect can be considered as a quadratic system described by [19]

$$y(t)=\alpha x(t)+\beta x^2(t), \tag{1}$$

where $x(t)$ is the input, $y(t)$ is the response, and α,β are constants. Suppose the input contains two sinusoids:

$$x(t)=A_1\ \sin\ (2\pi f_1 t+\phi_1)+A_2\ \sin\ (2\pi f_2 t+\phi_2), \tag{2}$$

where A_1, A_2, f_1 f_2 ϕ_1, and ϕ_2 are respectively the amplitudes, frequencies and initial phases of the two sinusoids. The corresponding response is

$$\begin{aligned} y(t)=&\alpha A_1\ \sin\ (2\pi f_1 t+\phi_1)+\alpha A_2\ \sin\ (2\pi f_2 t+\phi_2)\\ &-\beta\frac{A_1^2}{2}\cos\ [2\pi(2f_1)t+2\phi_1]\\ &-\beta\frac{A_2^2}{2}\cos\ [2\pi(2f_2)t+2\phi_2]+\beta A_1A_2\ \cos\ [2\pi(f_2-f_1)t\\ &+(\phi_2-\phi_1)]-\beta A_1A_2\ \cos\ [2\pi(f_2+f_1)t+(\phi_2+\phi_1)]. \end{aligned} \tag{3}$$

In the frequency domain, the above equation can be written as

$$\begin{aligned} Y(f)=&-i\frac{\alpha A_1}{2}\delta(f_1-f)e^{i\phi_1}-i\frac{\alpha A_2}{2}\delta(f_2-f)e^{i\phi_2}-i\frac{\beta A_1^2}{4}\delta(2f_1-f)e^{i\phi_1}\\ &-i\frac{\beta A_2^2}{4}\delta(2f_2-f)e^{i\phi_2}+i\frac{\beta A_1A_2}{2}\delta(f_2-f_1-f)e^{i(\phi_2-\phi_1)}\\ &-i\frac{\beta A_1A_2}{2}\delta(f_2+f_1-f)e^{i(\phi_2+\phi_1)}. \end{aligned} \tag{4}$$

As expected, the nonlinearity induces the interaction of ultrasonic waves, and generates harmonic waves at $2f_1$, $2f_2$ and sidebands at the sum and difference frequency f_1+f_2 and f_2-f_1. Note that the new spectral components (i.e., $f_3=f_1+f_2$) resulting from nonlinearity are phased coupled with the permanent interacting frequencies (i.e., f_1, f_2), which means that the sum of the phases at f_1 and f_2 is the phase at frequency f_3. This is known as quadratic phase coupling and can be considered an indication of second-order nonlinearities in the system.

The traditional linear power spectrum is the Fourier transform of the second-order cumulant, and carries no phase information. As a type of higher-order spectral density, the bispectrum is the Fourier transform of the third-order cumulant-generating function. Compared with linear power spectral analysis, the advantage of bispectral analysis is that it has the ability to characterize the quadratic phase coupling in monitored systems, and it has been applied successfully to evaluate the quadratic phase coupling types of nonlinear effects in mechanical systems [20].

For a stationary, random signal $x(t)$, the bispectral spectrum is given by

$$B(f_1,f_2)=E[X(f_1)X(f_2)X^*(f_1+f_2)], \tag{5}$$

where $X(f)$ is the Fourier transform of $x(t)$, $E[\,]$ indicates the expectation value and $*$ denotes the complex conjugate.

In practice, the expectation values in Eq. (5) need to be estimated from a finite quantity of available data. The estimated bispectrum of M separate databases is given by

$$\hat{B}(f_1,f_2)=\frac{1}{M}\sum_{i=1}^{M}X_i(f_1)X_i(f_2)X_i^*(f_1+f_2). \tag{6}$$

To more clearly describe the validity of the bispectrum for the characterization of quadratic phase coupling, we conduct bispectrum analysis on a signal similar to that described by Eq. (3), substituting ϕ_3 for $\phi_1+\phi_2$:

$$\begin{aligned} y(t)=&\alpha A_1\ \sin\ (2\pi f_1 t+\phi_1)+\alpha A_2\ \sin\ (2\pi f_2 t+\phi_2)\\ &-\beta\frac{A_1^2}{2}\cos\ [2\pi(2f_1)t+2\phi_1]\\ &-\beta\frac{A_2^2}{2}\cos\ [2\pi(2f_2)t+2\phi_2]+\beta A_1A_2\ \cos\ (2\pi(f_2-f_1)t\\ &+(\phi_2-\phi_1))-\beta A_1A_2\ \cos\ (2\pi(f_2+f_1)t+\phi_3). \end{aligned} \tag{7}$$

The bispectrum estimate of the above signal is then

$$\begin{aligned} \hat{B}(f_1,f_2)=&\frac{1}{M}\sum_{i=1}^{M}Y_i(f_1)Y_i(f_2)Y_i^*(f_1+f_2)\\ =&\frac{\alpha^2\beta}{8M}{A_1}^2{A_2}^2\sum_{i=1}^{M}e^{i(\phi_1+\phi_2-\phi_3)}. \end{aligned} \tag{8}$$

If the phase ϕ_3 is randomly distributed with respect to ϕ_1 and ϕ_2, then the summation in Eq. (8) sums components randomly distributed in phase and so tends to zero as $M\to\infty$. However, in the case that $\phi_3=\phi_1+\phi_2$, i.e. the three components are quadratically phase coupled, the resulting bispectrum is real-valued and nonzero, then the estimated bispectrum becomes

$$\hat{B}(f_1,f_2)=\frac{\alpha^2\beta}{8M}{A_1}^2{A_2}^2. \tag{9}$$

This allows detection of quadratically phase-coupled responses, and the bispectrum can be used to detect nonlinearity in systems (such as that induced by a defect). Therefore, the occurrence of sidebands at the sum or difference frequency in bispectral analysis can be taken as an indication of the presence of damage in the specimen and can be used as the basis of a nondestructive technique for damage detection.

3. Experiments and results

Micro-crack detection experiments were conducted using the collinear wave mixing technique. The Ritec Advanced Measurement SNAP 5000 system (RITEC Inc.) was used to conduct two types of experiments: measurements of the amplitudes of the mixing components at different frequencies or at different time delays, and measurements of the intermodulated waves at fixed frequencies and time delays.

3.1. Specimens and experimental setup

Experimental measurements were performed on a series of steel beams. Fig. 1 is a schematic diagram of the experimental system for the collinear wave mixing measurement.

The Ritec-SNAP system is the core component of the nonlinear measurement system. Two different frequency tone bursts are output from two 'RF burst' channels of the SNAP system, and used to drive two transducers (T1 and T2). A broadband piezoelectric transducer (T2) with central frequency of 4.000 MHz is used as both transmitter and receiver, and the other broadband piezoelectric transducer (T1) with central frequency of 2.000 MHz is used only for excitation. The excitations sent to both transducers are 20-cycle tone bursts of 1200 V but with different frequencies. The excitation sent to transducer T1 has a fixed frequency, $f_1 = 2.000$ MHz. The excitation sent to transducer T2 has a variational frequency f_2. Measurements are performed at varying frequency f_2 to generate both resonance and non-resonance conditions. As shown in Fig. 1, the interaction among the two incident waves and the nonlinearities in the sample generates a nonlinear ultrasonic response. Parts of the resultant waves are received by transducer T2. This function is enabled by a diplexer, which is connected to the input channel of the SNAP system.

In experiments of the nonlinearity measurement, the interested frequencies are usually different from the frequencies of the transmitted signal. Therefore, the receiving system must be capable of selecting specific frequencies of interest and rejecting others, which may be much larger in amplitude. The superheterodyne receiver of the SNAP system can detect the interested frequencies from the detected signals.

A set of steel beams was investigated as shown in Fig. 2. The beams were 156 mm long and had a cross-section of 34 mm × 17 mm. All beams were notched transversally in the middle by wire-electrode cutting. The length of a notch was 13 mm and the width was 1 mm. One beam was kept undamaged to be used as a reference. The remaining beams were fatigued at a rate of 10 cycles/s in a three-point bending rig. The pre-machined notch was used to initiate a micro-crack. The dynamic load is about 7.2 kN. The number of cycles is about 55×10^3. The length of the micro-crack was about 4 mm.

3.2. Experiments on the driving frequency

Experiments were conducted to investigate the effect of the driving frequency on the performance of collinear wave mixing. In these measurements, the driving frequency f_1 was fixed ($f_1 =$ 2.000 MHz) and the driving frequency f_2 varied around the resonance frequency from 2.7 MHz to 3.5 MHz. The amplitude of the sidebands at the sum and difference frequencies generated by wave fixing was measured by the superheterodyne receiver of the SNAP system, and is plotted in Fig. 3 as a function of driving frequency.

Fig. 3 shows that the variation tendencies of the amplitudes of the sidebands at sum and difference frequencies depend strongly on the damage condition of the samples. For the sample without a micro-crack, the amplitudes of the sidebands are quite small and almost independent of driving frequency; for samples with a micro-crack, the amplitudes of the sidebands are particularly sensitive to the driving frequency. It is noted that there are several local resonance points in the range of 2.95–3.10 MHz (as shown in the red dashed rectangle). In this range, the amplitudes of sidebands obtained from samples with a micro-crack are much larger than the amplitude of a sideband obtained from the sample without a micro-crack. It is seen that if the collinear wave mixing experiments are performed within this range, there might be significant interaction among the two waves and the micro-defect.

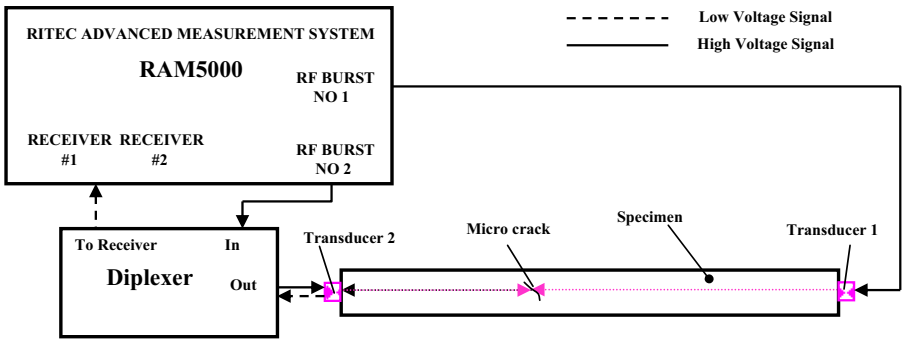

Fig. 1. Schematic diagram of the experimental system.

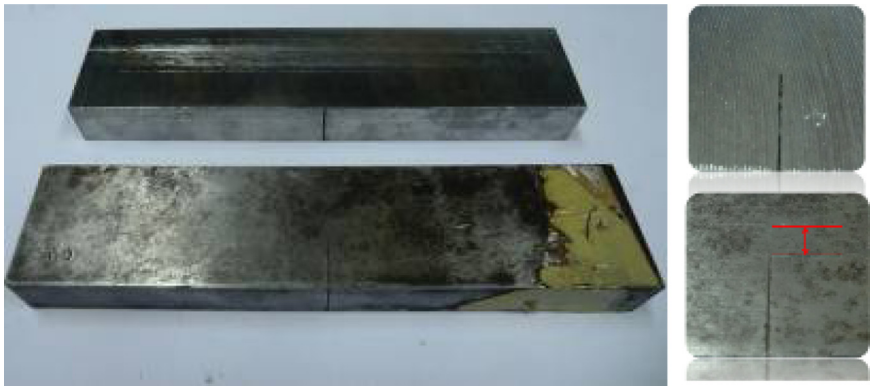

Fig. 2. Photograph of a specimen.

3.3. Results of bispectral analysis

To directly illustrate the effect of the driving frequency on the performance of collinear wave mixing, contrastive experiments were conducted for samples with and without a micro-crack at four pairs of driving frequencies: 2.000 MHz and 2.796 MHz, 2.000 MHz and 2.979 MHz, 2.000 MHz and 3.062 MHz, and 2.000 MHz and 3.360 MHz. The different driving frequencies f_2 were determined by considering the frequency dependence of the amplitudes of sidebands at sum and difference frequencies, and these frequencies are respectively shown by dash-dotted lines A–D in Fig. 3. It is seen that at line B (f_2=2.979 MHz), there is approximately the maximum difference in the amplitudes of the sidebands for two samples; at line D (f_2=3.360 MHz) there is no perceivable difference in the amplitudes of the sidebands; and at lines A and C (f_2=2.796 MHz and 3.062 MHz) there is some difference in the amplitudes of the sidebands.

Fig. 4 shows the typical responses when the driving frequencies are 2.979 MHz and 2.000 MHz. From the waveforms, it is difficult to discern whether there is quadratic phase coupling induced by nonlinearity. According to Eq. (6), the bispectra of the responses were calculated and their distributions in two and three dimensions are respectively shown in Figs. 5 and 6.

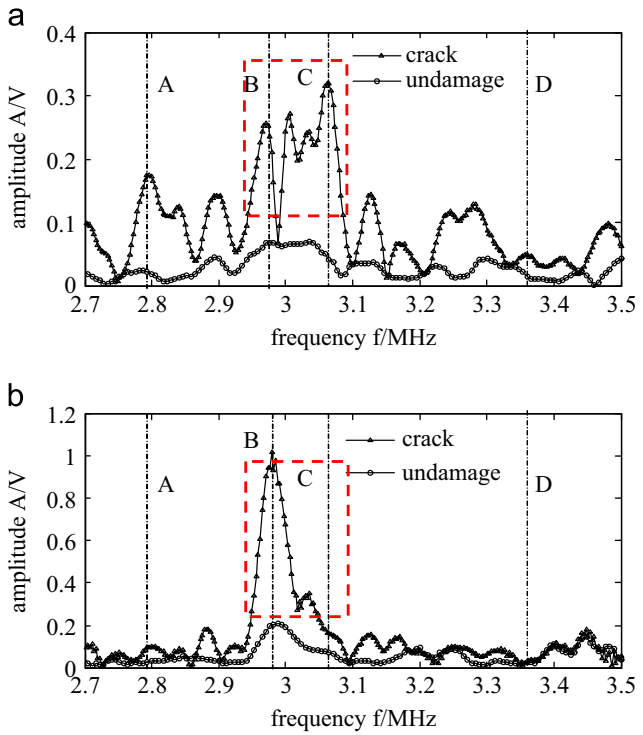

Fig. 3. Amplitude–frequency dependence of sidebands at sum and different frequency detected in samples with and without micro-crack when f_1 is 2.000 MHz, (a) at f_1+f_2, (b) at f_2-f_1.(For interpretation of the references to color in this figure legend, the reader is referred to the web version of this article.)

Figs. 5 and 6 show that, in each case, there are several peaks in the bispectrum, which are the only points where the bispectrum is nonzero. For example, in Fig. 5(c), there are altogether six peaks. Owing to the symmetry, the six peaks correspond to four features: the sideband at the difference frequency (B(f_1,f_2-f_1,f_2); labeled '1'), the sideband at the sum frequency (B(f_1,f_2,f_1+f_2); labeled '2'), and the two harmonics (peaks B(f_1,f_1,$2f_1$) and B(f_2,f_2,$2f_2$), labeled '3' and '4' respectively).

Fig. 5 shows an obvious difference in the number of bispectral peaks in the two cases. For samples with a micro-crack, there are bispectral peaks induced both by sidebands at sum and difference frequencies and by harmonics; however, for the sample without a micro-crack, there are only bispectral peaks induced by harmonics. It is seen that the occurrence of peaks at sum and difference frequencies in the bispectral distribution indicates the presence of micro damage in the specimen. Clearly, the collinear wave mixing method developed in this study provides a sensitive tool for micro-crack detection.

It is noted that the driving frequency strongly affects the amplitudes of the bispectral peaks. As shown in the three-dimensional distribution of the bispectrum (Fig. 6), when driving at 2.000 MHz and 2.979 MHz, the amplitude of the bispectral peaks reaches a maximum; when driving at 2.000 MHz and 3.360 MHz, the amplitudes of the bispectral peaks are a minimum; and in the other two cases, the amplitudes of bispectral peaks are mid-range. This variation in bispectral peak amplitude with driving frequency agrees well with the amplitude–frequency dependence of sidebands at sum and difference frequency shown in Fig. 3. The results indicate that the performance of the collinear wave mixing technique for the detection of a micro-crack is significantly affected by the driving frequency. The amplitude–frequency curves shown in Fig. 3 provide guidance for the determination of the driving frequency in a wave mixing measurement. The optimal driving frequency is such that the amplitudes of sidebands at both the sum and difference frequencies are a maximum.

It is worth noting that, in any case, there are bispectral peaks induced by harmonics. A reasonable explanation for this is that there are nonlinearities in the experimental system, such as those relating to transducers and amplifiers.

3.4. Results of defect location

According to the mechanism of collinear wave mixing, two wave packets will interact with defects only when they meet at the positions of defects. Therefore, in the experiments of collinear wave mixing with adjustment of the time delay of the excitations, the intersection of the two wave packets can be positioned along the whole length of the sample. Consequently, the nondestructive detection of the whole sample can be accomplished. Moreover,

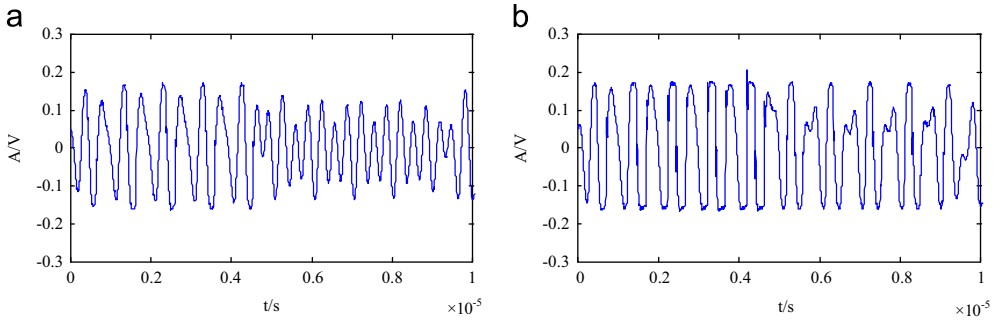

Fig. 4. Typical responses for driving frequencies of 2.979 MHz and 2.000 MHz. (a) sample without micro-crack. (b) sample with micro-crack.

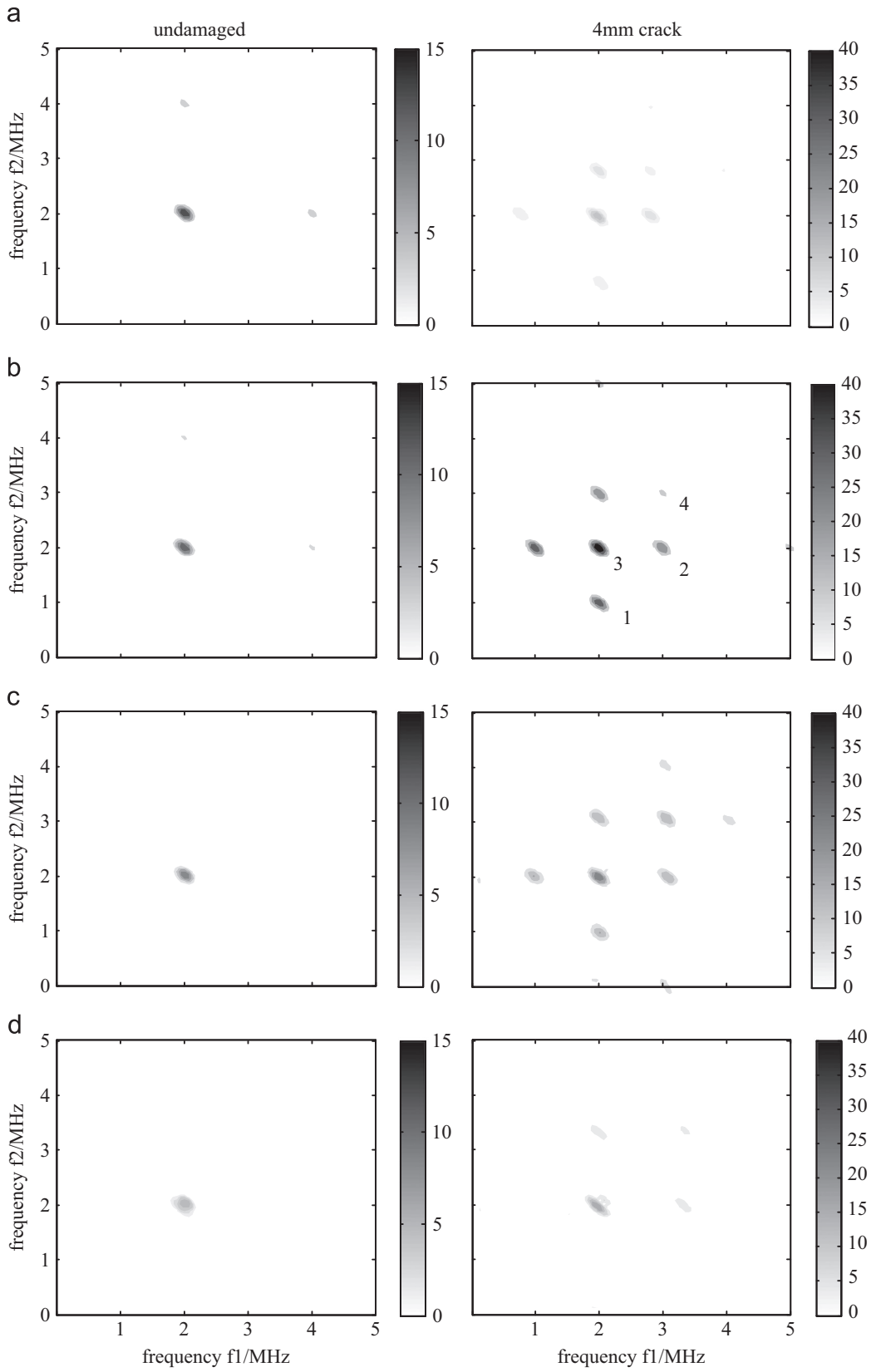

Fig. 5. Two-dimensional distribution of the bispectrum for two samples at different driving frequencies (a) 2.000 MHz and 2.796 MHz, (b) 2.000 MHz and 2.979 MHz, (c) 2.000 MHz and 3.062 MHz, (d) 2.000 MHz and 3.360 MHz.

according to the time-delay dependence of the amplitudes of mixing components, the location of the defect can also be determined.

In this part, experiments were conducted to investigate the effect of the time delay of excitation on the performance of collinear wave mixing. First, experiments were conducted on the

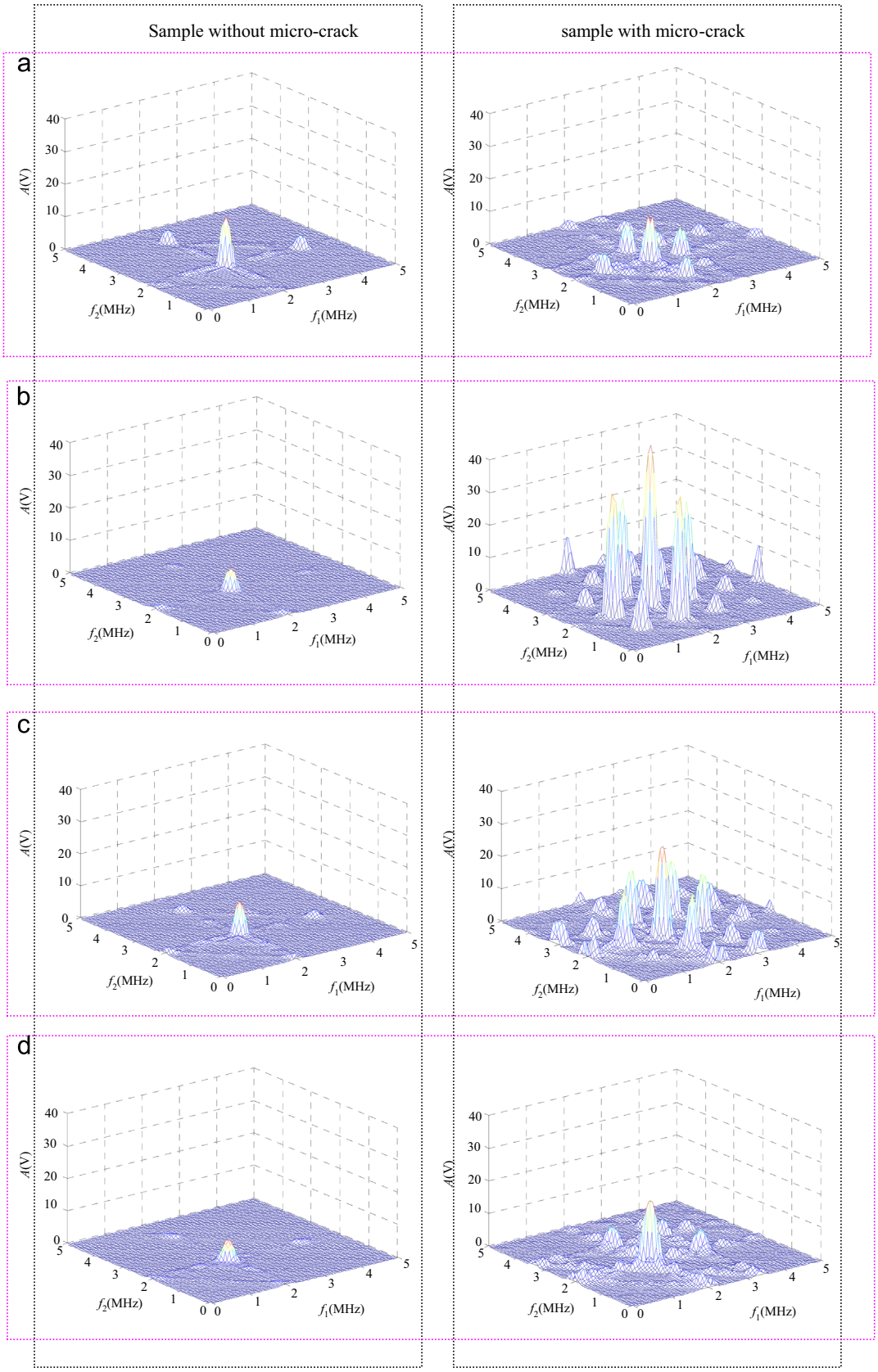

Fig. 6. Three-dimensional distribution of bispectrum for two samples at different driving frequency (a) (2.000 MHz, 2.796 MHz), (b) (2.000 MHz, 2.979 MHz), (c) (2.000 MHz, 3.062 MHz), (d) (2.000 MHz, 3.360 MHz).

same two samples as above. One had a micro-crack in the middle, and the other had no micro-crack in the middle. In these measurements, the excitation signals are 20-cycle tone bursts, and the driving frequencies f_1 and f_2 are respectively 2.000 MHz and 2.979 MHz. Therefore the durations of tone bursts are respectively 10 μs and 6.7 μs. The time-delay of RF BURST 1 was

fixed (30 μs), and the time-delay of RF BURST 2 varied continuously from 20 μs to 45 μs.

The amplitude of the sidebands at sum and difference frequencies generated by wave fixing was measured by the superheterodyne receiver in the SNAP system, and is plotted in Fig. 7as a function of time delay. Fig. 7 shows that the variation tendencies of the amplitudes of the sidebands at sum and difference frequencies depend strongly on the damage condition of the samples. For the sample without a micro-crack, the amplitudes of the sidebands are quite small and almost independent of the time delay; for the sample with a micro-crack, the amplitudes of the sidebands are particularly sensitive to the time delay. Obviously the amplitudes of sidebands obtained from samples with a micro-crack are much larger than those obtained from the sample without a micro-crack, and the amplitudes of sidebands from samples with a micro-crack reach maximum when the time delay of RF BURST 2 is closed to 30 μs.

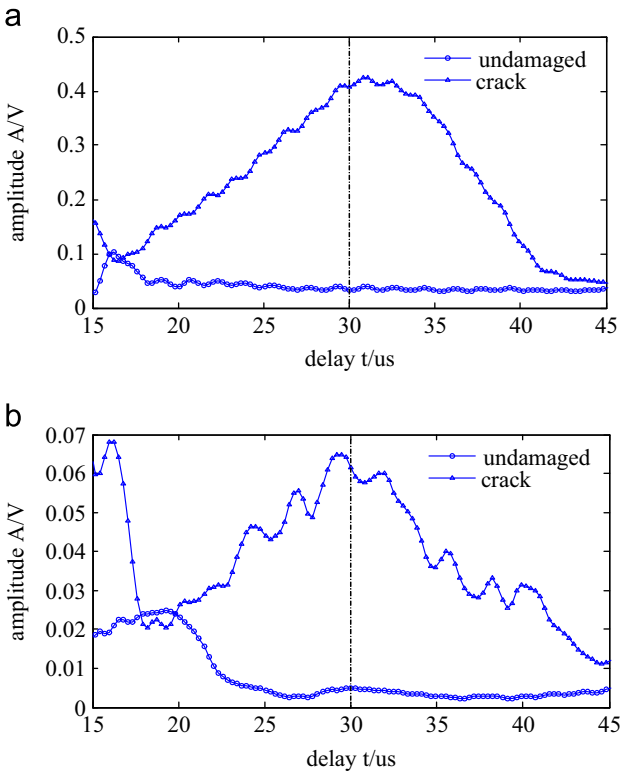

Fig. 7. Time-delay dependence of sidebands at sum and difference frequency detected in samples with and without micro-crack when time-delay of signal 1 is 30 μs (a) at f_1+f_2, (b) at f_2-f_1.

Since the time-delay of RF BURST 1 is 30 μs and the defect is located in the middle of sample, the intersection of the two wave packets occurs in the middle of the sample, therefore the time-delay dependence of the amplitude of sidebands at sum and difference frequencies can be used for defect location.

Due to the long durations of excitations, there are overlap regions for the two interfering wave packets at the defect location, which leads to the broadness of the peaks in Fig. 7. The overlap size is mainly related to the durations of tone bursts. Despite that, there is a slight difference between the time delays determined by two sidebands (29 μs and 31 μs), and both have trivial errors from 30 μs. This is possibly due to the long duration of tone bursts and the difference in frequency-tracking precision of the superheterodyne receiver. Meanwhile, it is noted that there is also a large amplitude peak when the time delay of RF BURST 2 is closed to 16 μs. The possible reason is that the two waves meet at the contact interface of the transducer and sample, which is obviously another kind of nonlinear source.

To validate the sidebands-based measurement techniques for defect location, time delay dependence of sidebands at sum and difference frequency was measured on another three steel samples with micro-cracks at different positions. The beams are 240 mm long, and have a cross-section of 24 mm × 48 mm. All beams were also fatigued by cyclic loading, and the length of the micro-crack was about 3 mm. In three beams the distances between the micro-cracks and right end of beam are respectively 90 mm, 105 mm, 120 mm. The time-delay of RF BURST 1 was fixed (15 μs), and the time-delay of RF BURST 2 varied continuously from 2 μs to 30 μs. Fig. 8 shows the typical results, and Table 1 provides details of the test results. It is clear that the time delay corresponding to the maximum amplitude of sidebands can be used to calculate the location of defects. Although the time delays determined by two sidebands are not identical, the deviation from the theoretical values is quite small.

4. Conclusion

This paper developed a collinear wave mixing technique for the detection of micro-cracks in metal samples. The technique measures the mixing of two ultrasonic sinusoidal waves that are excited by two transducers mounted bilaterally on a sample. The Ritec Advanced Measurement SNAP 5000 system was used in two series of experiments-tracking of the mixing components versus frequency or time delay, and measurement of the ultrasonic intermodulation at fixed frequencies and time delay—and the nonlinear response was processed using the well-known bispectrum method. It was found that the occurrence of peaks at sum and difference frequencies in the bispectral distribution indicates

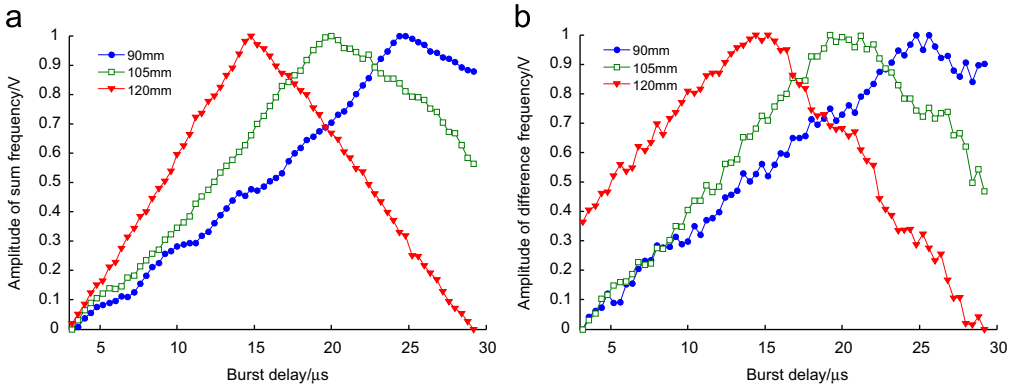

Fig. 8. Time-delay dependence of sidebands at sum and difference frequency detected in samples with micro-cracks at different locations when time-delay of signal 1 is 15 μs. (a) at f_1+f_2. (b) at f_2-f_1.

Table 1
Comparison between time delays determined by two sidebands.

Number of experiments	**Distance:90 mm** **Time delay** (μs)			**Distance:105 mm** **Time delay** (μs)			**Distance:120 mm** **Time delay** (μs)		
	Sum frequency	Difference frequency	Theoretical value	Sum frequency	Difference frequency	Theoretical value	Sum frequency	Difference frequency	Theoretical value
1	25.2	25.2	25.2	20.4	19.6	20.1	15.2	14.8	15.0
2	25.6	25.4		19.8	20.6		15	15	
3	25	26		19.8	20		14.8	15.6	
4	25.8	26		19.8	20.6		15.4	15.6	
5	25.4	25.4		19.8	20.6		15.2	15.6	

the presence of micro damage in the specimen. Therefore, the collinear wave mixing method developed in this study provides a sensitive tool for micro-crack detection. Moreover, the driving frequency strongly affects the performance of the collinear wave mixing technique for micro-crack detection, and the optimal driving frequency is such that the amplitudes of both the sum and difference frequency sidebands reach a maximum. The time delay of excitations determined whether the ultrasonic waves meet at the location of a defect, which is essential for ultrasonic intermodulation. According to the time-delay dependence of the amplitude of mixing components, the technique of collinear waves mixing can be used to locate defects throughout a sample.

Since the proposed method detects and locates the defects by measuring the amplitude of mixing components, it is less sensitive to linear sources in structures, such as boundary, open-cracks etc., thus it has potential application in geometrically complex components.

Acknowledgements

This work was supported by the National Natural Science Foundation of China (grant nos. 51075012 and 11272017), the Beijing Natural Science Foundation (grant no. 1122005) and National "Twelfth Five-Year" Plan for Science & Technology Support (201110032, 2011BAK06B03-03).

References

[1] Donskoy D, Sutin A, Ekimov A. Nonlinear acoustic interaction on contact interfaces and its use for nondestructive testing. J NDT and E Int 2001;34(4):231–8.
[2] Jhang K-Y. Nonlinear ultrasonic techniques for nondestructive assessment of micro damage in material: a review. Int J Precis Eng Manuf 2009;10(1):123–35.
[3] Jeong H, Nahm SH, Jhang KY, Nam YH. A nondestructive method for estimation of the fracture toughness of CrMoV rotor steels based on ultrasonic nonlinearity. Ultrasonics 2003;41(7):543–9.
[4] Jhang KY. Applications of nonlinear ultrasonics to the NDE of material degradation. IEEE Trans Ultrason Ferroelectr Freq Control 2000;47(3):540–8.
[5] Van Den Abeele KE-A, Carmeliet J, Ten Cate JA, Johnson PA. Nonlinear elastic wave spectroscopy (NEWS) techniques to discern material damage, Part II: Single-mode nonlinear resonance acoustic spectroscopy. Res Nondestr Eval 2000;12(1):31–42.
[6] Kim J, Jacobs L, Qu J. Experimental characterization of fatigue damage in a nickel-base superalloy using nonlinear ultrasonic waves. J Acoust Soc Am 2006;120(3):1266–73.
[7] Novak A, Bentahar M, Tournat V, El Guerjouma R, Simon L. Nonlinear acoustic characterization of micro-damaged materials through higher harmonic resonance analysis. NDT and E Int 2012;45:1–8.
[8] Sutin AM, Johnson PA. Nonlinear elastic wave NDE II. Nonlinear wave modulation spectroscopy and nonlinear time reversed acoustics. In: AIP conference proceedings; 2005.760(I1). p.385–392.
[9] Jacob X, Catheline S, Gennisson J-L, Barrière C. Nonlinear shear wave interaction in soft solids. J Acoust Soc Am 2007;122(4):1916–25.
[10] Zaitseva V, Nazarova V, Gusevb V, Castagnede B. Novel nonlinear-modulation acoustic technique for crack detection. NDT and E Int 2006;39:184–94.
[11] Huang D, Rose A, Poutrina E, Poutrina Ekaterina, Larouche S, David RS. Wave mixing in nonlinear magnetic metacrystal. Appl Phys Lett 2011;98 (204102–1-3).
[12] Croxford AJ, Wilcox PD, Drinkwater BW. The use of non-collinear mixing for nonlinear ultrasonic detection of plasticity and fatigue. J Acoust Soc Am 2009;126(5):117–22.
[13] Croxford AJ, Drinkwater BW, Wilcox PD. Nonlinear ultrasonic characterization using the noncollinear. AIP Conf Proc 2011;1335:330–7.
[14] Demcenko A, Akkerman R, Nagy PB, Loendersloot R. Non-collinear wave mixing for non-linear ultrasonic detection of physical ageing in PVC. NDT and E Int 2012;49:34–9.
[15] Jacob X, Barriere C, Roye D. Acoustic nonlinearity parameter measurements in solids using the collinear mixing of elastic waves. Appl Phys Lett 2003;82(6):886–8.
[16] Liu M, Tang G, Jacobs LJ, Qu J. Measuring acoustic nonlinearity parameter using collinear wave mixing. J Appl Phys 2012;112:024908.
[17] Hills AJ, Neild SA, Drinkwater BW, Wilcox PD. Global crack detection using bispectral analytics. Proc R Soc London, Ser A 2006;462:1515–30.
[18] Hills AJ, Neild SA, Drinkwater BW, Wilcox PD. Bispectral analysis of ultrasonic inter-modulation data for improved defection detection. Rev Quant Nondestr Eval 2006;25:89–96.
[19] Courtney CRP, Neild SA, Wilcox PD, Drinkwater BW. Application of the bispectrum for detection of small nonlinearities excited sinusoidally. J Sound Vib 2010;29:4279–93.
[20] Countney CRP, Drinkwater BW, Neild SA, Wilcox PD. Factors affecting the ultrasonic intermodulation crack detection technique using bispectral analysis. J NDT and E Int 2008;41(3):223–34.